Bulgarian Chemical Communications, Volume 50, Special Issue A (pp. 171- 176) 2018

High voltage cathode materials based on lithium cobaltate with nickel and manganese doping

K. Banov[1,2], T. Petkov[2], R. Boukoureshtlieva[1], D. Ivanova[2], L. Fachikov[2], V. Kotev[4], B. Banov[* 1,3]

[1]*Institute of Electrochemistry and Energy Systems, IEES, Acad. G. Bonchev str., bl. 10, 1113 Sofia*
[2]*University of Chemical Technology and Metallurgy – UCTM, bul. "Kl. Ohridski" N:8, 1756 Sofia*
[3]*European Polytechnical University – EPU, 23, "St. St. Cyril and Methodius" str., 2300 Pernik*
[4]*Institute of Mechanics, IM, 1,Acad. G. Bonchev str., bl. 4, 1113 Sofia*

Received July14, 2017; Accepted October 20, 2017

Doped lithium cobaltates $LiCo_{1-y}M_yO_2$ (M = Mn, Ni, y = 0.1, 0.3, 0.5) have been prepared by low temperature solid-state reaction. The structure of the samples was characterized by X-ray diffraction (XRD). The specific surface area (SSA) of the materials was examined by B.E.T. method. The synthesized powders were found to have rhombohedral structure, except for $LiCo_{0.5}Mn_{0.5}O_2$, which crystallises with cubic spinel-like structure (space group Fd3m). The electrochemical performances of the compounds were studied by galvanostatic cell cycling in the high-voltage range between 3.0 and 4.8 V vs. Li/Li^+ electrode. It was shown that the type and the amount of the doping element greatly affect the structure, electrochemistry and cycle life characteristics of the investigated materials. $LiCo_{0.9}Mn_{0.1}O_2$ has shown better cycling results compared to all other compounds.

Keywords: High voltage cathodes; cobaltate and nickelate doped with manganese, NMC cathodes.

INTRODUCTION

Lithium cobalt oxide ($LiCoO_2$) is the most commonly used positive electrode material in commercial lithium-ion batteries due to its high energy density, high working voltage and good thermal and structural stability during cycling [1,2]. The theoretical capacity of $LiCoO_2$ is 274 mAh g^{-1} however its practical capacity attainable is only about 140 $mAhg^{-1}$ when cycled in the voltage range of 3.0 - 4.3 V. By increasing the cut off voltage, the energy density of the cell can be increased by ~ 15%. However, the cyclability of $Li_{1-x}CoO_2$ rapidly deteriorates for x > 0.5 (i.e. above 4.3 V) due to crystallographic phase transitions and the associated unit cell volume changes [3]. Moreover, the formed Co^{4+} ions with their strong oxidative character lead to dissolution of the electrolyte on the particle surface, resulting in considerable gas release, which is responsible for the capacity fade and mechanical failure of the cells. [4, 5].

Doping with metal ions is an effective approach, which has been applied to stabilize the layered structure of the cathode material allowing good reversibility at high voltages and increasing the capacity of the system $LiCo_{1-y}M_yO_2$ (M = metal) [6, 7]. Theoretical studies indicate that transition metal doping of $LiCoO_2$ leads to an increased capacity, while non-transition metal doping can increase the voltage at the expense of the capacity. Different metal substituents like Fe, Mn, Ni, Al, Mg [8-12] at the Co – site in $LiCoO_2$ have been studied with respect to possible improvement in the electrochemical performance of the material.

In the present study, we report on the synthesis of doped lithium cobaltates $LiCo_{1-y}M_yO_2$ (M = Mn, Ni). The compounds have been obtained by solid-state method at relatively low temperatures with respect to the classic solid-state reactions using also alternative precursors and optimising the synthesis conditions. The materials were subjected to structural and electrochemical characterization in order to study their potential use as high-voltage cathode materials in lithium-ion batteries.

EXPERIMENTAL

The phases $LiCo_{1-y}M_yO_2$ (M = Mn, Ni, y = 0.1, 0.3, 0.5) were synthesized by solid-state method using nitrate precursors: $LiNO_3$, $Co(NO_3)_2.6H_2O$, $Mn(NO_3)_2$ and $Ni(NO_3)_2.6H_2O$ (Merck). The stoichiometric amounts of the precursors were mechanically homogenized in a ball mill for 1 h. Ten percent excess of $LiNO_3$ was added to the mixtures in order to avoid the loss of Li as Li_2O. The obtained powders were initially heat treated in an oven at 450^0C for 24 h following by additional grounding for 2 h in a ball mill. Further the samples were annealed in air at 650^0C for 12 h. The mixture was cooled, mixed thoroughly and subjected to physical and electrochemical characterizations. Powder X-ray diffraction (XRD) patterns of the phases were

* To whom all correspondence should be sent.
E-mail: bbanov@iees.bas.bg

© 2018 Bulgarian Academy of Sciences, Union of Chemists in Bulgaria

RJ Technology Exhibit 2035
Apple Inc. v. RJ Technology LLC
IPR2023-01183, Page 1 of 6

obtained using a Philips APD-15 diffractometer with CuKα radiation, internal Si standard and computer data management. The lattice parameters were calculated using the dependence between the Miller indices (hkl) and d-spacing, with the program UNIT CELL - TJB Holland & SAT Redfern method (1995) applying the least-squares method. The Specific Surface Area (SSA) of the samples was determined by B.E.T. (Brunauer-Emmet-Teller) method by means of BET areameter Stroehlein (Germany). The electrochemical characterizations were carried out using a three-electrode metal cell fully modelling a coin cell 2032 with the advantage of lithium reference electrode. The electrolyte consisted of a solution of 1M $LiPF_6$ + 0.2M $LiClO_4$ in EC (ethylene carbonate) : DMC (dimethyl carbonate) : DEC (diethyl carbonate) in 1:1:1 volume ratio. The composite test electrode materials were a mixture of the compounds studied with Teflonized Acetylene Black (TAB-2) at 8:2 ratio by weight. The prepared mix was coated onto an aluminium foil that served as a current collector by applying 10 t cm^{-2} pressures using a hydraulic press. The cells were assembled in an argon-filled glove box and were subjected to galvanostatic charge-discharge cycling tests. The electrochemical tests were performed on a computer controlled multi-channel battery-cycling device at a current rate of 0.2C in the voltage range of 3.0-4.8 V at room temperature.

RESULTS AND DISCUSSIONS

Structural characterization

$LiCo_{1-y}Mn_yO_2$ cathode materials

Fig. 1. shows the X-ray diffraction patterns of $LiCo_{1-y}Mn_yO_2$ (y = 0.1, 0.3, 0.5) samples synthesized by solid-state method and calcined at 650^0C. It can be seen that all compositions do not form a single phase. The existence of secondary phases, which can be indexed to Co_3O_4 and MnO_2 is observed. The intensity of the peak at $2\theta = 36.8^0$ corresponding to Co_3O_4 phase increases considerably with increasing the Mn content to y = 0.3 (Fig. 1b). In the XRD patterns of $LiCo_{0.9}Mn_{0.1}O_2$ and $LiCo_{0.7}Mn_{0.3}O_2$ (Fig. 1a, b) it can be observed that the fingerprint peaks, (003), 101, 006, 102, 104, 108 and 110 are clearly identifiable thereby suggesting the existence of hexagonal lattice structure of the α-$NaFeO_2$ type (R-3m space group). With increasing the Mn amount to y = 0.5 the crystal structure is changed and the X-ray patterns of $LiCo_{0.5}Mn_{0.5}O_2$ can be indexed to a cubic unit cell (fcc) of the spinel-type structure (space group Fd3m). These results confirm the reports available in the literature about Mn doped lithium cobaltates [10, 13].

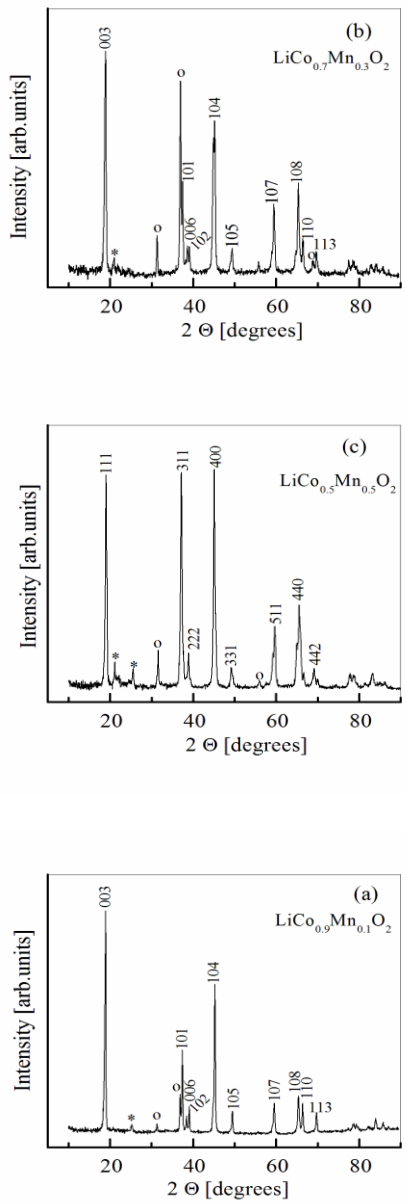

Fig.1. XRD patterns of a) $LiCo_{0.9}Mn_{0.1}O_2$, b) $LiCo_{0.7}Mn_{0.3}O_2$ and c)$LiCo_{0.5}Mn_{0.5}O_2$ powders prepared by low temperature solid-state method at 650^0C. Secondary phases in the powders are indexed to Co_3O_4 (○) and MnO_2 (*).

The unit cell parameters of all $LiCo_{1-y}Mn_yO_2$ compositions calculated from the XRD patterns are listed in Table 1. The results indicate that the hexagonal-close packed lattice is maintained only for y = 0.1 and y = 0.3. The values of the lattice parameters for these samples are slightly larger than those reported for pure $LiCoO_2$ [14-18]. With increasing content of the Mn-dopant, both the metal-metal intrasheet distance (*a*) and the metal-metal interlayer distance (*c*) increase. The substitution of Mn for Co leads to expansion of the unit cell parameters and overall cell volume, which is in tune

RJ Technology Exhibit 2035
Apple Inc. v. RJ Technology LLC
IPR2023-01183, Page 2 of 6

with the ionic radii of the elements (Co^{3+} = 0.545 Å, Mn^{3+} = 0.67 Å) [19]. As can be seen in Table 1, the c/a ratio of 4.99 indicates a well-defined layered structure and an ordered distribution of lithium and transition-metal ions in the lattice. The ratio of intensities of the XRD lines $I_{(003)}/I_{(104)}$ is considered as an indicator of the ordering of the lithium and transition metal ions [20]: the larger the ratio, the better expressed layered structure.

Table 1. Structural data of the compounds $LiCo_{1-y}Mn_yO_2$ (y = 0.1, 0.3, 05)

Material	Structural data						
	Space group	(a) [Å]	(c) [Å]	c/a	U. cell vol. [Å^3]	$I_{(003)}/I_{(104)}$	Crystal Size [nm]
$LiCo_{0.9}Mn_{0.1}O_2$	R3m	2.8131	14.0480	4.99	96.2753	1.49	30
$LiCo_{0.7}Mn_{0.3}O_2$	R3m	2.8190	14.0685	4.99	96.8188	1.44	21
$LiCo_{0.5}Mn_{0.5}O_2$	Fd3m	8.0826			528.0240		20

The $I_{(003)}/I_{(104)}$ values are more than unity for y = 0.1 and y = 0.3 (Table 1) suggesting the formation of ordered layered structure. The well defined doublets (006) /(102) and (108)/(110) observed in XRD patterns of $LiCo_{0.9}Mn_{0.1}O_2$ support this conclusion. On the other hand, the (108) peak of the (108)/(110) doublet is higher in the pattern of $LiCo_{0.7}Mn_{0.3}O_2$ (Fig. 1b), which could be discerned as an indication of possible inhomogeneous distribution of Mn and Co ions in the structure. Based on the structural data it can be expected that $LiCo_{0.9}Mn_{0.1}O_2$ will exhibit better electrochemical behaviour. The average crystallite size *L*of the doped materials was calculated from X-ray data applying Debye-Scherer equation [21]. As can be seen from Table 1 the mean crystallite size of the $LiCo_{1-y}Mn_yO_2$ materials decreased with increasing the amount of the manganese component. The same tendency was observed for the Specific Surface Area (SSA) of the compounds. The largest SSA was obtained for the sample $LiCo_{0.9}Mn_{0.1}O_2$ (3.48 m^2 g^{-1}), while the materials with y = 0.3 and y = 0.5 showed SSA of 1.90 m^2 g^{-1} and 1.78 m^2 g^{-1}, respectively.

$LiCo_{1-y}Ni_yO_2$ cathode materials

The XRD patterns of the synthesized $LiCo_{1-y}Ni_yO_2$ (y = 0.1, 0.3, 0.5) materials are shown in Fig. 2. All diffraction peaks could be indexed based on a hexagonal α-$NaFeO_2$ structure with a space group of R-3m. The patterns appear to be similar to those reported for pure layered $LiCoO_2$ [22]. There is a clear splitting of the (006)/(102) and (108)/(110) doublet peaks, which indicate uniform ordering of lithium and transition-metal ions in the structure [13].

Table 2. Structural data of the compounds $LiCo_{1-y}Ni_yO_2$(y = 0.1, 0.3, 05)

Material	Structural data					
	(a) [Å]	(c) [Å]	c/a	U. cell vol. [Å^3]	$I_{(003)}/I_{(104)}$	Crystal Size [nm]
$LiCo_{0.9}Ni_{0.1}O_2$	2.8128	14.0296	4.99	96.1280	1.35	27
$LiCo_{0.7}Ni_{0.3}O_2$	2.8133	14.0404	4.99	96.2338	1.12	30
$LiCo_{0.5}Ni_{0.5}O_2$	2.8139	14.0487	4.99	96.2765	1.11	31

All peaks are sharp and well defined suggesting that materials are well crystallized. In all spectra the presence of some extra peaks due to impurities of NiO are observed. The hexagonal cell parameters of the doped compounds, calculated from the XRD spectra, are given in Table 2.

The results show that the hexagonal-close-packed lattice is preserved for all samples. With increasing the amount of the doping element a slight increase of the lattice parameters (*a*) and (*c*) can be seen, since the ionic radius of Ni^{3+} (0.69 Å) is larger than that of Co^{3+} (0.545 Å). The intensity ratio $I_{(003)}/I_{(104)}$ exceeds unity, which is a further evidence of the cation ordering in the obtained structures.

This is confirmed also by the values of the (*c/a*) ratio, which is higher than 4.90, corroborating the layered structure of the materials. As seen in Table 2, the $I_{(003)}/I_{(104)}$ ratio decreases with increasing the Ni content in $LiCo_{1-y}Ni_yO_2$ samples, which indicates that higher Ni concentrations could result in probable cation mixing in the structure. In contrast with the Mn doped compounds the mean crystallite size of $LiCo_{1-y}Ni_yO_2$ powders increases with increasing the Ni content. Subsequently a slight increase of the measured SSA can be observed in the order $LiCo_{0.9}Ni_{0.1}O_2$ (1.72 m^2 g^{-1}) <$LiCo_{0.7}Ni_{0.3}O_2$ (1.81 m^2 g^{-1}) <$LiCo_{0.5}Ni_{0.5}O_2$ (1.88 m^2 g^{-1}).

RJ Technology Exhibit 2035
Apple Inc. v. RJ Technology LLC
IPR2023-01183, Page 3 of 6

Electrochemical characterization

The electrochemical performance of the prepared cells was evaluated galvanostatically by cycling the cells from 3.0 to 4.8 V. The cells exhibited an open circuit voltage of around 3.0 V (vs. Li metal). In Fig.3 the discharge curves of Li//$LiCo_{1-y}Mn_yO_2$ and Li//$LiCo_{1-y}Ni_yO_2$ cells recorded at C/5 rate are presented *(5 hours discharge rate according to the theoretical capacity value of used cathode material)*. As the manganese doping content increased from x = 0.1 to 0.5 significant decrease of the discharge voltage is observed (Fig.3a), which is in accordance with the theoretic calculations of Ceder et al. and Venkatraman et al. [4, 7, 23], concerning the effect of Co substitution (partly or completely) with 3d metal in $Li_{1-x}(Co_{1-y}M_y)O_2$ at given *x*.

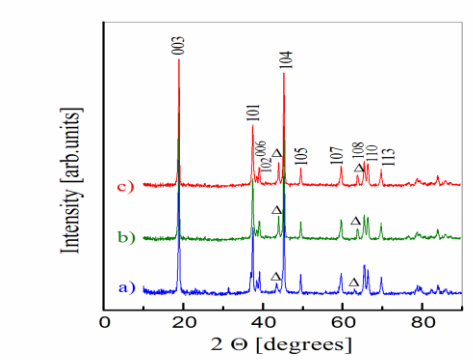

Fig. 2. XRD patterns of a) $LiCo_{0.9}Ni_{0.1}O_2$, b) $LiCo_{0.7}Ni_{0.3}O_2$ and c)$LiCo_{0.5}Ni_{0.5}O_2$ powders prepared by low temperature solid-state method at 650^{0}C. The impurity peaks are indicated as NiO (Δ).

All doped materials exhibit a potential slightly lower than for the pure $LiCoO_2$ phase, which could be attributed to the different morphology and structure changes during cycling. For the Ni doped compounds, the increase of the Ni mol part does not change the discharge plateau (Fig. 3b), which is due to the fact that Co and Ni can be substituted mutually without changing the $LiCoO_2$ structure.

Besides the discharge plateau at 3.8 V a second discharge plateau at about 4.4 V in both doped materials, $LiCo_{1-y}Mn_yO_2$ and $LiCo_{1-y}Ni_yO_2$, can be observed, which is attributed to second lithiation process. The dependence of the specific capacity on the number of the cycles is presented on Fig. 4.

It can be seen that $LiCo_{0.9}Mn_{0.1}O_2$ shows comparatively high initial capacity of 140 mAh g^{-1} and very good cycling stability (Fig. 4a), which means that doping with 10 mol % Mn stabilizes the structure of the lithium cobaltate.

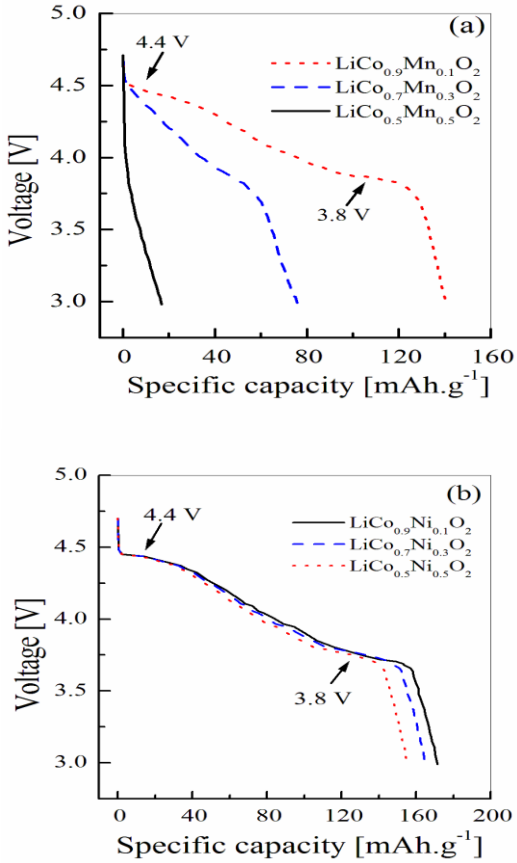

Fig.3. Discharge curves of the compounds (a) $LiCo_{1-y}Mn_yO_2$ (y = 0.1, 0.3, 0.5) and (b) $LiCo_{1-y}Ni_yO_2$ (y = 0.1, 0.3, 0.5) in the voltage window 3.0 – 4.8 V

However the discharge capacities of the $LiCo_{1-y}Mn_yO_2$ (y = 0.1, 0.3, 0.5) materials decreased with increasing the Mn content. The results of the electrochemical testing of the compound consisted of equal amounts of transition elements ($LiCo_{0.5}Mn_{0.5}O_2$) show that it possesses low electrochemical activity, which may be due to the structural change of the material. In contrast to the Mn doped compounds, in case of $LiCo_{1-y}Ni_yO_2$ the increase of the Ni content leads to a considerable increase of the initial capacity of the material, reaching 170 mAh g^{-1} for $LiCo_{0.5}Ni_{0.5}O_2$ (Fig. 4b). Similar increase of the starting capacity when doping with Ni is reported also by Li et al. [24]. However, at the same time the stability during cycling deteriorates, which could be due to a kinetic problem – it is known that some of the $LiCo_{1-y}Ni_yO_2$ phases are low electron conductors.

Another possible explanation could be the occupation of Li sites in the structure by Ni ions, which hinders the lithiation-delithiation process.

RJ Technology Exhibit 2035
Apple Inc. v. RJ Technology LLC
IPR2023-01183, Page 4 of 6

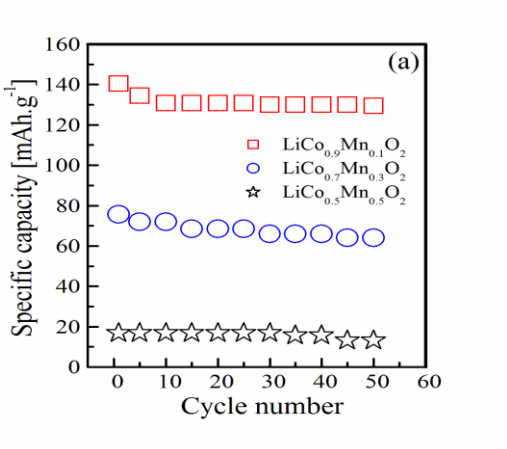

Fig.4. Plots of specific capacity versus cycle number for the compounds (a) $LiCo_{1-y}Mn_yO_2$ and (b) $LiCo_{1-y}Ni_yO_2$ in the voltage window 3.0 – 4.8 V

The presence of cation mixing can be confirmed also by the X-ray patterns. The increased Ni content leads to a decrease of the intensity ratio of the diffraction lines (003) and (104), reflecting an increased Ni content at the Li sites, which correspondingly results in deteriorated cycling stability of all Ni doped compounds. From all materials under investigation $LiCo_{0.9}Mn_{0.1}O_2$ shows the best electrochemical behaviour due to its structural and morphological properties. Its intensity ratio $I_{(003)}/I_{(104)}$ of the material is 1.49, i.e the highest value in comparison to the other doped materials. $I_{(003)}/I_{(104)}$ ishigher than unity suggesting the formation of well ordered layered structure. $LiCo_{0.9}Mn_{0.1}O_2$ is characterized also with the largest SSA, which considerably influenced its electrochemical performance.

CONCLUSIONS

Doped lithium cobaltates $LiCo_{1-y}M_yO_2$ (M = Mn, Ni; y = 0.1, 0.3, 0.5) were synthesized by solid-state method from nitrate precursors. The effect of Mn and Ni doping on the structural and electrochemical properties of the materials was investigated. XRD analysis shows that the layered structure of lithium cobaltate is preserved up to doping with 50 mol % Ni and about 30 mol % of Mn. We demonstrated that $LiCo_{0.9}Mn_{0.1}O_2$ synthesized in this way is a promising cathode material for use in lithium-ion batteries, delivering capacities of 130 mAh g^{-1} at a 0.2C rate when cycled in the high voltage range (4.8V). Moreover, it possesses very good cycling stability in the extended galvanostatic cycling studies (50 cycles). Doping with 10, 30 and 50 mol % Ni results in an increased initial capacity (by 20 %), but also leads to deterioration with cycling.

REFERENCES

1. K. Mizushima, P.C. Jones, P.J. Wiseman, J.B. Goodenough, *Solid State Ionics*, **3-4**, 171 (1981).
2. J. M. Tarascon, M. Armand, *Nature*, **414**, 359 (2001).
3. S. Levasseur, M. Menetrier, E. Suard, C. Delmas, *Solid State Ionics*, **128**, 11 (2000).
4. G. Ceder, Y.-M. Chiang, D.R. Sadoway, M.K. Aydinol, Y.-I. Jang, B. Huang, *Nature*, **392**, 694 (1998).
5. G. G. Amatucci, J.M. Tarascon, L.C. Klein, *Solid State Ionics*, **83**, 167 (1996).
6. Ceder, G.; Chiang, Y. M.; Sadoway, D. R.; Ayginol, M. K.; Jang, Y. I.; Huang, B. *Nature*, **392**, 894(1998).
7. S. Venkatraman, V. Subramanian, S. Gopu Kumar, et. al., *Electrochem. Commun.*, **2,** 18 (2000).
8. H. Kobayashi, M. Shigemura, H. Tabuchi, K. Sakaebe, H. Ado, A. Kageyama, R. Hirano, M. Kanno, S. Wakita, S. Morimoto, S. Nasu, *J. Electrochem. Soc*., **147**, 960 (2000).
9. M. Holzapfel, R. Schreiner, A. Ott, *Electrochim. Acta*, **46**, 1063 (2001).
10. R. Stoyanova, E. Zhecheva, L. Zarkova, *Solid State Ionics*, **73**, 233 (1994).
11. C. Delmas, I. Saadoune, A. Rougier, *J. Power Sources*, **44**, 595 (1993).
12. C. Julien, *Solid State Ionics*, **157**,57 (2003).
13. Ch. Julien, *Solid State Ionics*, **135**, 241 (2000).
14. G. G. Amatucci, J.M. Tarascon, L. Klein, *J. Electrochem. Soc*., **143**, 1114 (1996).
15. H. J. Orman, P. J. Wiseman, *Acta Crystallogr.*, **C 40**,12 (1984).
16. J. Akimoto, Y. Gotoh, Y. Oosawa, *J. Solid State Chem.*, **141**, 298 (1998).
17. A. Marini, V. Berbenni, V. Massarotti, D. Capsoni, E. Antolini, *J. Solid State Chem.*, **116**, 23 (1995).
18. R. J. Gummow, M. M. Thackeray, W. I. F. David, S. Hull, *Mater. Res. Bull*., **27**, 327 (1992).
19. R. D. Shannon, Acta Crystallogr., **A32,** 751 (1976).
20. R. J. Gummow and M. M. Thackeray, *J. Electrochem. Soc.*, **140**, 3365 (1993).
21. P. Scherrer, GottingerNachrichtenGesell., 2 (1918) 98; A. L. Patterson, Phys. Rev., 56 (1939) 97
22. Ueda, T. Ohzuku, *J. Electrochem. Soc.*, **141**, 2013 (1994).
23. S. T. Myung, N. Kumagai, S. Komaba, H.T. Chung, *Solid State Ionics*, **139**, 47 (2001).
24. Chi-lin Li, W. Liu, Z. Fu, *Chinese J. of Chemical Physics*, **19,** 493 (2006).

RJ Technology Exhibit 2035
Apple Inc. v. RJ Technology LLC
IPR2023-01183, Page 5 of 6

ВИСОКО ВОЛТОВИ КАТОДНИ МАТЕРИАЛИ НА ОСНОВАТА ЛИТИЕВ КОБАЛТАТДОТИРАНИ С НИКЕЛ И МАНГАН

Кр. Банов[1,2], Т. Петков[2], Р. Букурещлиева[1], Д. Иванова[2],
Л. Фачиков[2], В. Котев[4], Бр. Банов[1,3*]

[1).] Институт по електрохимия и енергийни системи, ИЕЕС, ул. "Акад. Г. Бончев" N:1, Бл. 10. 1113 София
[2)] Химико-технологичен и металургичен университет, бул. "Кл. Охридски" N:8, 1756 София
[3)] Европейски политехнически университет, ЕПУ, ул. "Св. Св. Кирил и Методи" N:23, 2300 Перник
[4)] Институт по механика, ул. "Акад. Г. Бончев" N:1, Бл. 4. 1113 София

Постъпила на 14юли, 2017 г.; приета на 20 октомври, 2017 г.

(Резюме)

Дотиран с никел и манган литиев кобалтат $LiCo_{1-y}M_yO_2$ (M = Mn, Ni, y = 0.1, 0.3, 0.5) е синтезиран успешно по твърдофазен метод. Получените проби са охарактеризирани с помощта на рентгеноструктурен анализ. Специфичната повърхност е определена с помощта на BET метода. Изготвените проби притежават ромбоедрична структура с изключение на $LiCo_{0.5}Mn_{0.5}O_2$, която кристализира в кубична шпинелна структура от пространствена група **Fd3m.** Електрохимичното поведение на синтезираните материали е изследвано в електрохимична клетка при галваностатичен режим във високо волтовата област с граници 3.0V до 4.8V спрямо Li/Li^+ сравнителен електрод. Проведените изследвания показват, че количеството на дотиращия елемент определят в голяма степен структурата, електрохимичното поведение, и живота на изследваното съединение. Литиев кобалтат дотиран с манган с формула $LiCo_{0.9}Mn_{0.1}O_2$ показа най-добрите резултати по отношение на циклируемост в сравнение с другите изследвани съединения.

Ключови думи*:* високо волтови катоди за литиево йонни батерии, кобалтат и никелат дотирани с манган, катоди на основата на литиран никел манган кобалтови смесен оксид

RJ Technology Exhibit 2035
Apple Inc. v. RJ Technology LLC
IPR2023-01183, Page 6 of 6